

NUMERICAL STUDY OF COMPRESSED CO₂ PIPELINE DECOMPRESSION CHARACTERISTICS USING CFD-DECOM

Baopeng Xu, Hongen Jie and Jennifer X. Wen*

Centre for Fire and Explosion Studies, Faculty of Engineering, Kingston University London SW15, 3DW, UK

Russell Cooper and Julian Barnett

National Grid, Warwick Technology Park, Gallows Hill, Warwick, CV34 6DA, UK

*Correspondence: j.wen@kingston.ac.uk

A CFD based pipeline blowdown model has been developed and validated against experimental data for rich gas, gaseous and dense phase carbon dioxide. The multi-component fully compressible two-phase solver is coupled with the homogeneous equilibrium model which assumes that the two phases share identical velocity, temperature and pressure. Real gas behavior is considered by two equations of state. The liquid-vapour phase equilibrium of a multi-component rich gas is determined by flash calculations. A conjugate heat transfer problem is solved simultaneously for the pipe flow and wall heat transfer. The conserved transport equations are solved using an Arbitrary Lagrangian-Eulerian method. Predictions carried out for some previously tested blowdown scenarios are found to be in reasonably good agreement with the experimental data.

KEYWORDS: Carbon dioxide, rich gas, blowdown, CFD, homogeneous equilibrium model

INTRODUCTION

There is a growing world-wide interest for carbon capture and storage (CCS) as an approach to mitigate global warming. Such technique involves the transport of compressed vapour, liquid, dense phase CO₂ and CO₂/hydrocarbon gas mixtures via pipelines and process systems. Therefore the need has arisen to address the risk of potential loss of containment scenarios that can be environmentally damaging. A key issue is the possible formation, rain-out, and subsequent sublimation of solid CO₂.

CO₂ can be transported over long distances through pipelines either as dense phase fluid or as a gas. In the former, the relatively high density of CO₂ can help to ensure a high throughput. CO₂ pipelines are susceptible to long running ductile fractures (Cosham et al., 2008), in which extensive plastic deformation takes place before fracture. The Battelee two-curve model (TCM) is often used to determine the toughness required to arrest a running ductile fracture in a pipeline (Cosham et al., 2007). The key input to the TCM is the decompression curve, a relationship between the pressure and velocity of the pressure wave, which is highly dependent on the thermodynamic properties of the fluid, its initial pressure and temperature. For methane, the decompression curve is essentially a smooth curve regardless of the initial conditions. However, for rich gases and CO₂, this often contains a plateau due to the discontinuity in the speed of sound caused by the phase transition (Cosham et al., 2007; Botrosa et al., 2007). The existence of the plateau in the decompression curve will result in higher toughness requirement for the pipeline according to the TCM based design calculations.

Apart from the early work of Maxey (1986), there is virtually no experimental data within the public domain about the decompression behaviour of either gaseous or dense phase CO₂, whilst such information is urgently required to inform pipeline design in future CCS projects.

In this paper, we present ongoing work at Kingston University to develop CFD-DECOM, a predictive tool based on computational fluid dynamics (CFD) techniques for predicting the decompression behaviour of rich gas, gaseous and dense phase CO₂. The predictions will be compared with the measurements of Maxey (1986) and the predictions of Cosham and Eiber (2007) using GASDECOM. In the absence of further experimental data for CO₂, the predictions have also been compared with previously measured decompression curves for several rich gases with slightly different compositions. On this basis, we present the predictions of the model for different CO₂ release conditions.

NUMERICAL FORMULATION AND SOLUTION PROCEDURE

CONSERVATION EQUATIONS

For the homogeneous equilibrium method (HEM) of two-phase flow, the two-phase mixture is assumed to be locally in thermodynamic and kinetic equilibrium, i.e. sharing the same velocity, temperature and pressure. Therefore, the two-phase mixture can be treated as a pseudo-fluid governed by the same conservation equations as a single-phase flow. The conservation equations of multi-component two-phase mixture can be described in vector notation with bold symbols representing vector and tensor quantities as follows:

$$\text{Total mass equation: } \frac{\partial \rho}{\partial t} + \nabla \cdot (\rho \mathbf{u}) = 0 \quad (1)$$

where ρ is total mass density, t time and \mathbf{u} fluid velocity.

Mass equation for species m :

$$\frac{\partial \rho_m}{\partial t} + \nabla \cdot (\rho_m \mathbf{u}) = \nabla \cdot \left[\rho D \nabla \left(\frac{\rho_m}{\rho} \right) \right] \quad (2)$$

where ρ_m is mass density of species m , D diffusion coefficient.

Momentum equation:

$$\frac{\partial(\rho \mathbf{u})}{\partial t} + \nabla(\rho \mathbf{u} \mathbf{u}) = -\nabla p + \rho \mathbf{g} \quad (3)$$

where p is fluid pressure and \mathbf{g} gravity.

Total energy equation:

$$\frac{\partial(\rho E)}{\partial t} + \nabla \cdot (\rho \mathbf{u} E) = -\rho \nabla \cdot \mathbf{u} - \nabla \cdot \mathbf{J} \quad (4)$$

where E is total energy, $E = 1 + \frac{1}{2} \mathbf{u} \cdot \mathbf{u}$, I specific internal energy, \mathbf{J} heat flux vector, $\mathbf{J} = -k \nabla T - \rho D \sum_m h_m \nabla \left(\frac{\rho_m}{\rho} \right)$, k thermal conductivity, T fluid temperature and h_m specific enthalpy of species m .

Heat transfer and wall friction are not explicitly included in the energy and momentum equations as source terms, but will be treated as boundary conditions. The inclusion of species equations makes treatments of multi-component mixture and varied species concentration resulting from species mixing and stratification possible.

To close the equations (1)–(4), an equation of state (EOS) is required. Two equations of state, Peng-Robinson (1976) and Span Wanger (1996), are implemented in CFD-DECOM. The Peng-Robinson EOS, which is widely used in the petro-chemical industry, is adopted to calculate the thermodynamic properties and phase equilibrium data coupled with a mixing rule (Robert et al., 1987) for rich gas mixtures as well as CO₂. The Span Wanger EOS was especially developed for carbon dioxide and known to provide more accurate predictions for CO₂ thermodynamic properties and phase equilibrium data than the Peng-Robinson EOS. Comparison will be made for the predictions of CO₂ decompression using the two EOSs.

The thermodynamic variables ρ , and I are the properties of the two-phase pseudo-fluid mixture expressed as:

$$\frac{1}{\rho} = x \frac{1}{\rho_g} + (1-x) \frac{1}{\rho_l} \quad (5)$$

$$I = x I_D + (1-x) I_l \quad (6)$$

where the subscriptions of l and g respectively stand for saturated liquid and vapour which can be individually multi-component mixture and x is quality of the two-phase mixture. The liquid-vapour phase equilibrium of multi-component rich gas is determined by flash calculations using the method of the reference (Mehra et al., 1983). This is a computational process of determining equilibrium composition and mole fraction of each phase in a multi-component multiphase system. In this study, only flash calculations under constant temperature and pressure is required.

BOUNDARY CONDITIONS

Two types of wall boundary conditions are implemented. For multi-dimensional simulations, a wall function (Amsden et al., 1989) (not used in current study) is used to compute wall heat transfer and friction. For one-dimensional simulations, empirical correlations are often employed to compute wall friction and wall heat transfer. The treatment of wall friction of two-phase mixture for one-dimensional simulations is similar to that of single phase flow calculations.

The friction factor for single phase is given by (Massey, 1983):

$$C_f = \frac{16}{Re} \quad \text{for } Re < 2000$$

$$C_f = 0.001375 \left[1 + \left(2000 \frac{\varepsilon}{d} + \frac{10^6}{Re} \right)^{1/2} \right]$$

for $Re \geq 2000$ (7)

where ε is pipeline roughness and $Re = \rho u d / \mu$, d is pipeline inner diameter. For two-phase wall friction, ρ is taken as density of two-phase mixture and viscosity of two-phase mixture is calculated according to (Beattie, 1982) by $\mu = (1-\alpha)(1+2.5\alpha)\mu_l + \alpha\mu_g$, where α is void fraction and related to quality x by $x = \frac{Mw_l \cdot (1-\alpha)}{Mw_l \cdot (1-\alpha) + Mw_v \cdot \alpha}$ where Mw_l is molecular weight for liquid phase and Mw_v for gas phase. The viscosity of carbon dioxide in liquid and gas phase is calculated using correlations in Vesovic (1990) and Fenghour (1998). The viscosity of the rich gas is determined according to Vesovic (2001).

For one-dimensional simulations, a conjugate two-phase wall heat transfer model similar to Fairuzov's approach (2000) is implemented. A separate heat transfer problem is simultaneously solved for the solid wall with the flow solver. The heat transfer equation is given by:

$$\rho_s c_s \frac{\partial T}{\partial t} = \nabla \cdot (k_s \nabla T) \quad (8)$$

where, ρ_s , c_s and K_s are density, specific heat and heat conductivity of solid wall. The coupling of the solid phase solver with the flow solver is achieved at the inner wall boundary by satisfying:

$$K_s \frac{\partial T_s}{\partial n} \Big|_{r=w} = h(T_w - T_f) \quad (9)$$

where n is the normal to the wall, T_s solid temperature, T_w wall temperature, T_f fluid temperature and h heat transfer coefficient of forced convection at inner wall. The heat transfer coefficient is calculated according to empirical correlations (Chen, 1966; Chen, 1961). Equation (8) is discretized using a finite volume method and solved by a conjugate residual method (O'Rourke, 1986).

For problems of full-bore blowdown, an outflow boundary is needed at the rupture plane. Choked flow is

Table 1. Test conditions and composition for rich gas cases

Cases	P [MPa]	T [k]	Composition [mol%]									
			CO2	N2	CH4	C2H6	C3H8	iC4	nC4	iC5	nC5	nC6
1	10.58	247.56	0.781	0.569	95.474	2.936	0.19	0.016	0.025	0.004	0.003	0.002
2	20.545	248.35	0.764	0.566	95.127	3.288	0.204	0.017	0.027	0.004	0.003	0.002
3	14.21	277.76	0.642	0.457	76.493	16.627	5.745	0.012	0.017	0.003	0.002	0.002
4	9.949	268.16	0.553	0.408	68.509	21.406	9.08	0.026	0.014	0.002	0.002	0.001

quickly established at the rupture plane following the rupture. Similar to our previous study (Wen, 2009), sudden release is assumed to start from still and an infinitely fast rupture rate is assumed. Prior to the establishment of sound speed at the outflow boundary, the pressure at the outflow plane is interpolated from a combination of the inner cell pressure next to the outflow plane and ambient pressure which is normally the atmospheric pressure. As the choked flow from the sudden release develops, the downstream disturbance cannot propagate upstream to influence the upstream pipe flow. Therefore, the pressure at the outflow boundary is only interpolated from the inner cell pressures if the outflow velocity is equal to its local speed of sound. With this technique, a choked condition can be assumed at the rupture plane during the blowdown process.

NUMERICAL METHODS

A finite volume method is employed to integrate equations (1)–(4). The conservation equations are discretized on staggered mesh with velocity stored on cell vertices and thermodynamic variables namely density and temperature and pressure at cell centers. All computational cells are three-dimensional arbitrary hexahedrons which allow for handling complex geometries. Volume integrals are converted to surface integrals according to divergence theorem. The discretization of the governing equations is conducted using an Arbitrary Lagrangian-Eulerian method (ALE) (Hirt et al., 1974). In the ALE approach, the convective terms are solved separately from the other terms, for instance pressure gradient in the momentum equation. Each computational time step is divided into two phases: a Lagrangian phase and a rezone phase. In the Lagrangian phase, computational grids move with fluid velocity, so the convection terms are not solved. A second-order Crank-Nicolson time scheme is used for the diffusion terms and the terms associated with pressure wave propagation, which are spatially discretized using a second-order central scheme. The coupled semi-implicit equations in the Lagrangian phase are solved by a SIMPLE type algorithm with individual equations solved by a conjugate residual method (O'Rourke and Amsden, 1986) and a Poisson equation is solved for pressure. In the rezone phase, the computational grids are moved back to their original locations and convective fluxes are computed. The convective fluxes are calculated in a sub-cycled explicit manner

(Amsden, 1989) using a sub-time step that is an integral sub-multiple of the main computational time step. The sub-time step satisfies the Courant condition, so the limit of time step on CFL can be relaxed and computational efficiency is increased. Two convection schemes are implemented: a quasi-second-order upwind (QSOU) (Amsden, 1989) and an upwind WENO scheme (Balsara and Shu, 2000) which is more accurate for flows involving shock waves.

VALIDATIONS

DECOMPRESSION WAVE VELOCITY

As a pipeline ruptures, a leading decompression wave propagates away from the rupture plane into the undisturbed compressed fluid at the local speed of sound. Behind the leading decompression wave, the decompression wave velocity is equal to the local speed of sound minus local escaping velocity. Close to the rupture plane, the decompression rate is fast, so the effect of heat transfer and wall friction are negligible and the decompression process can be assumed to be isentropic. With this assumption, the decompression wave velocity is only a function of local pressure for a specific blowdown. Further away from the rupture plane, the decompression rate gradually slows down, the effect of heat transfer and wall friction become relatively more important and can no longer be neglected. Therefore, the decompression wave velocity is not only a function of local pressure but also dependent on the local position along a pipeline.

The decompression curve, or more precisely the decompression wave velocity versus pressure, is an important factor for fracture analysis of pipelines (Maxey et al., 1975). The proposed methods in Section 2 are firstly validated against published experimental data on decompression curves (Botrosa et al., 2007; Maxey et al., 1975). All the experimental data in this section was measured at locations

Table 2. Test conditions for CO₂ cases

Cases	P [MPa]	T [k]	Phase
5	12.0622	299.82	Liquid
6	6.3773	296.26	Liquid
7	9.3291	307.59	Supercritical
8	14.5402	315.37	Supercritical

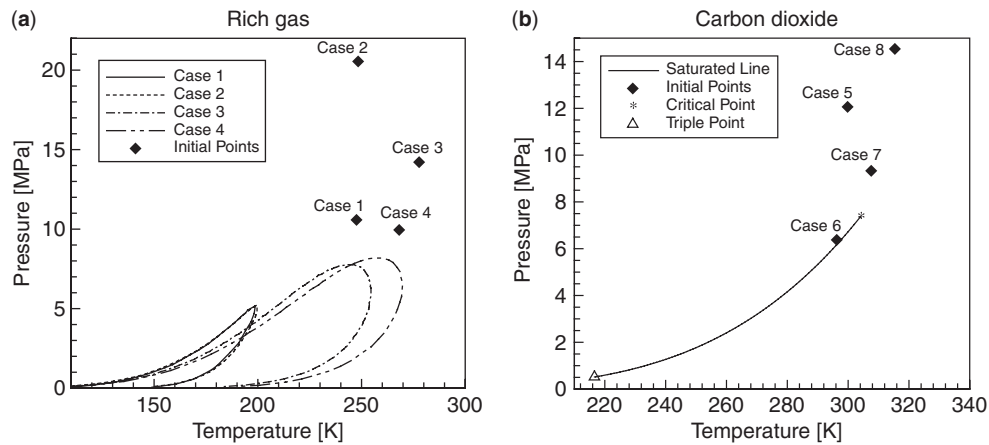


Figure 1. Initial release points and phase diagrams

close to the rupture plane, so the decompression wave velocity was assumed to be only a function of local pressure.

To simplify the problem, the following assumptions were made for the predictions: 1) the rupture rate is infinitely fast; 2) the decompression flow is one-dimensional;

3) the flow is isentropic by neglecting heat transfer and wall friction; 4) two-phase mixture is homogeneous and in thermodynamic and mechanical equilibrium. All the validation cases and test conditions are listed in Table 1 for rich gas cases (Botrosa et al. 2007) and Table 2 for CO₂

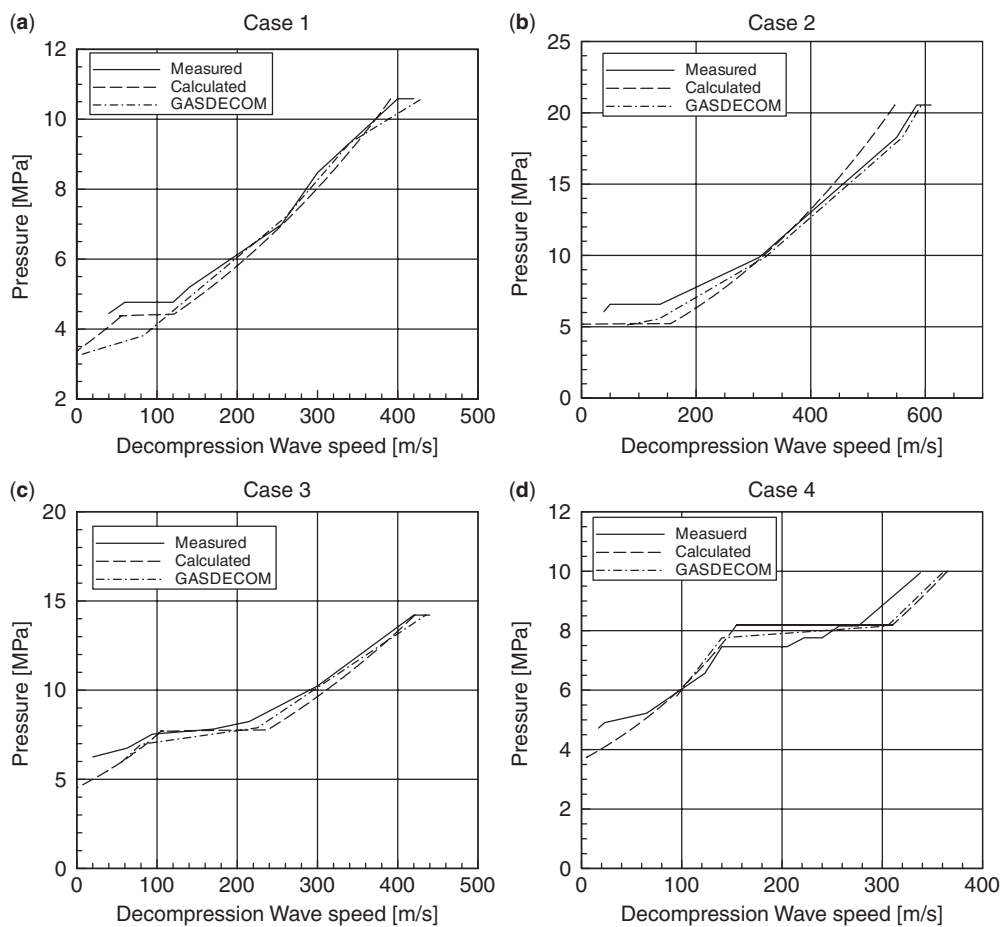


Figure 2. Decompression curves for the rich gas cases

cases (Maxey, 1986), and plotted in the corresponding phase diagram in Figure 1.

All the decompression curves start from the leading decompression wave ahead of which is the undisturbed compressed fluid at initial conditions. Therefore, the highest points in the decompression curves correspond to the initial pressure and speed of sound. A smooth section is observed on the decompression curve immediately after the initial decompression point. For this section, the fluid element starts to exit the pipe and there is no phase transition. Depending on the initial conditions, the decompression path may enter a two-phase region. The speed of sound is discontinuous across the phase transition and drops sharply for a two-phase mixture. The discontinuity in the speed of sound across the phase boundary results in a “plateau” on the decompression curves. After the phase transition, the decompression velocity gradually drops to zero at the choked rupture plane.

The comparison of the present predictions with the experimental data and the predictions of GASDECOM (1993) for the rich gas cases are presented in Figure 2. Overall, the present predictions are very close to the

predictions by GASDECOM and agree well with the experimental data. Both the present model and GASEDECOM are based on the homogeneous equilibrium assumption. Although the predictions are in reasonably good agreement with the experimental data, there are some discrepancies. Two major assumptions made in the simulations are most likely responsible for the discrepancies, i.e. the HEM assumption and the infinitely fast rupture rate. The experimental measurements were measured close to the rupture plane where non-equilibrium conditions might prevail to affect the validity of the HEM assumption. If non-equilibrium conditions prevail, the phase transition would take place at a pressure lower than the thermodynamic equilibrium pressure. The actual rupture process has a finite rupture rate, i.e. the full-bore rupture is achieved during a time period in which the release flow at the rupture plane is also three-dimensional. In consideration of the finite rate rupture, the outflow rate is smaller than the infinitely fast rate rupture during the very early stage of the release. This may also account for some of the discrepancies.

The comparison for the carbon dioxide cases are shown in Figure 3. All the four cases are for decompression

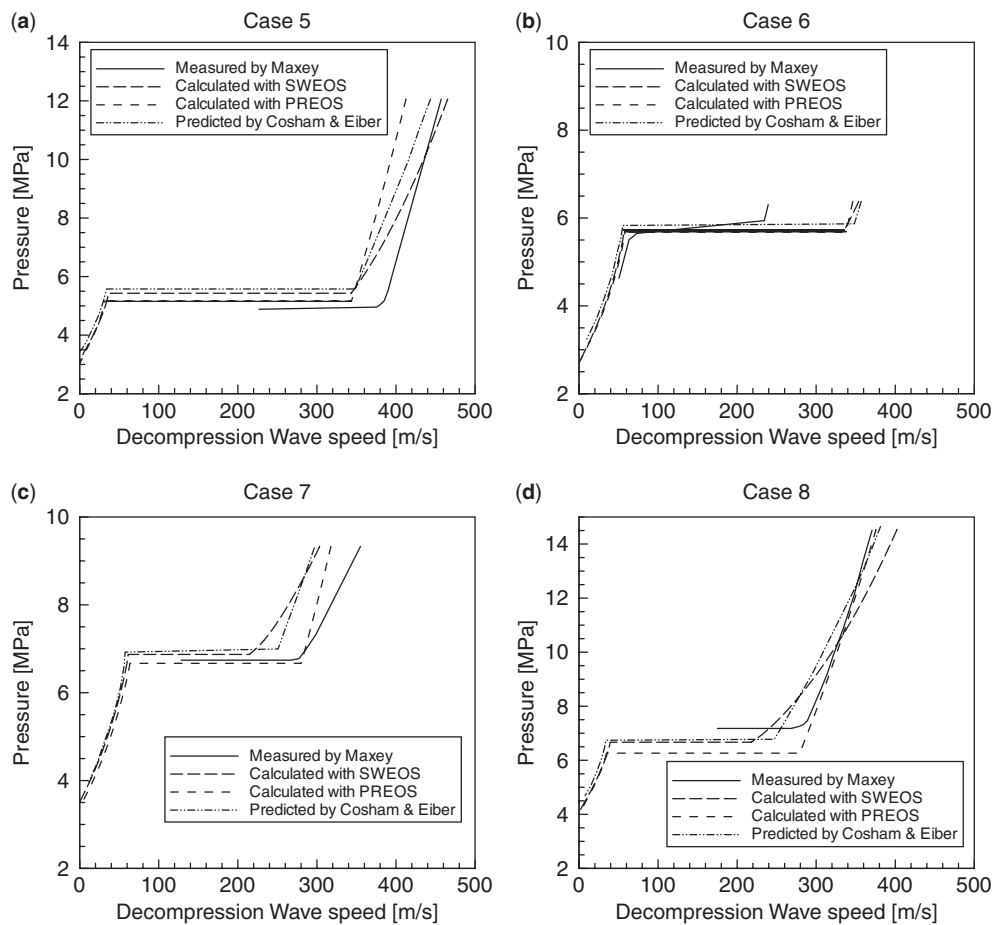


Figure 3. Decompression curves for the carbon dioxide cases

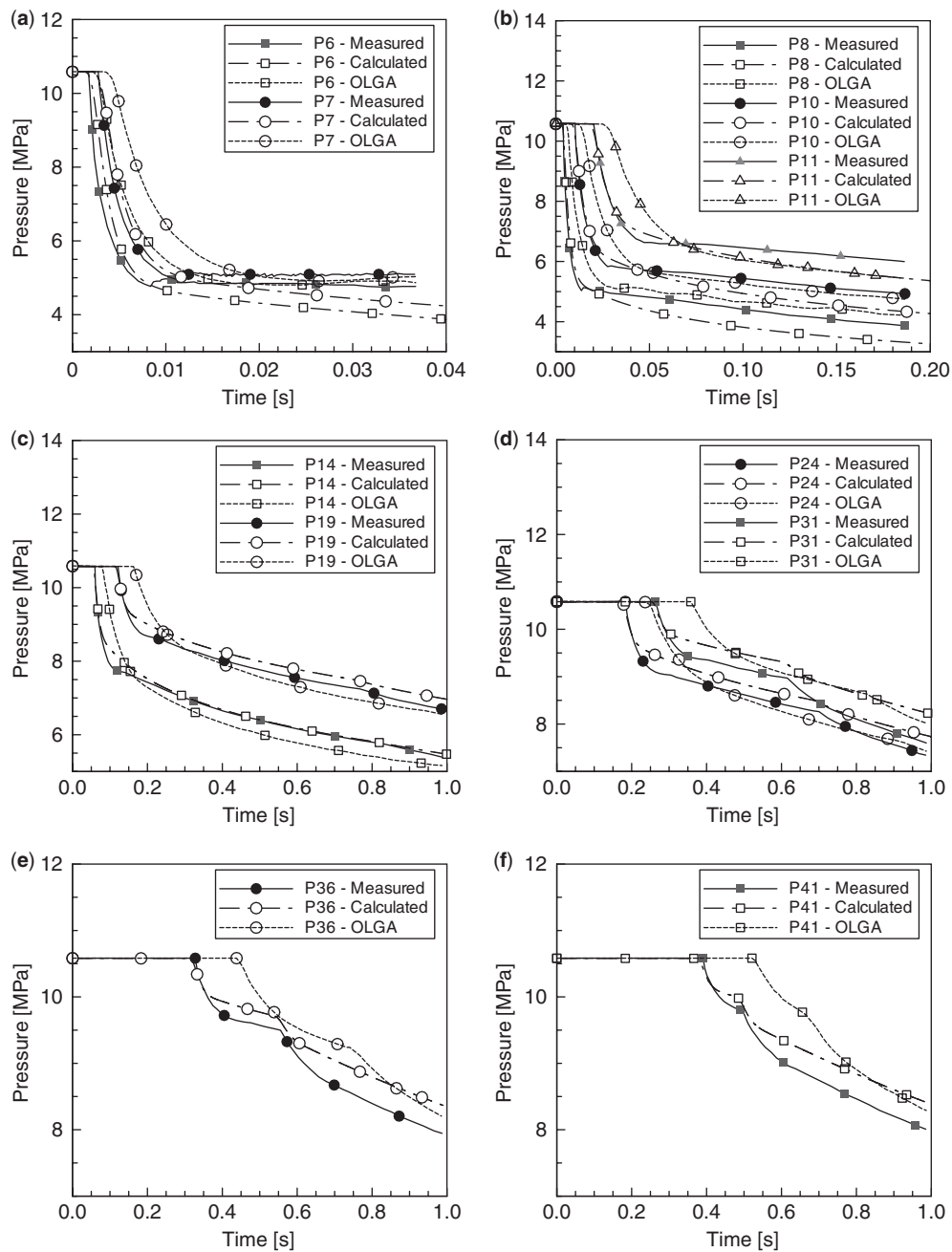


Figure 4. Comparison of pressure-time traces at different locations (case 1)

of liquid/supercritical carbon dioxide. The predictions by Cosham and Eiber (2008) using GASDECOM are also included for comparison. Good agreement is achieved for the predictions of the plateau pressure, while apparent differences in the predictions of sound speed for the liquid and supercritical phases exist as reflected by the differences in the predictions of the widths and positions of the plateaus by different models. The three equations of state, i.e.

Peng-Robinson (1976), Span-Wagner (1996) and BWRS (Prausnitz et al., 1987) all behave differently. The discrepancies are due to the small compressibility of carbon dioxide in liquid and supercritical phases. Speed of sound for single phase or two-phase mixture is expressed by

$$\alpha^2 = \left(\frac{\partial P}{\partial \rho} \right)_s \quad (10)$$

Table 3. Measurement locations for the rupture of rich gas

Node	6	7	8	10	11	14	19	24	31	36	41
Location [m]	0.84	1.24	1.64	4.04	8.04	23.06	47.07	71.09	103.16	127.17	151.19

where s is entropy and for two-phase mixture it can be calculated by

$$s = xs_g + (1 - x)s_l \tag{11}$$

An analytical solution is difficult to derive for equation (10), so the speed of sound is normally numerically computed by

$$\alpha^2 = \left(\frac{\Delta P}{\Delta \rho} \right)_s \tag{12}$$

and ΔP is taken as $0.001P$ in this study. Because of the small compressibility, $\Delta \rho$ is sensitive to the choice of equation of state, which causes the discrepancies.

PRESSURE/TEMPERATURE-TIME TRACES

In this section, validation is carried out against the experiments of Botros (2007) by comparison of pressure-time

and temperature-time traces at different locations along the pipeline. The test pipe is 172 m long and 4.9 cm in diameter. Only one test case (Case 1 Table 1) is compared here.

A conjugated problem is solved simultaneously for the pipe flow and wall heat transfer. The pipe flow is assumed to be one-dimensional, while two-dimensional heat conduction is solved for the pipe wall. Because the conservation equations are written in three-dimensional form, the computational domain is taken as a slice of the whole cylindrical pipe with an azimuthal angle of 0.5 degree. The front and back of the slice are set as periodic boundary conditions. The variable gradients in the radial direction are neglected, so only one cell was set in this direction for the fluid domain. The wall temperature gradient in the radial direction is much larger and needs to be resolved. The grid sensitivity study demonstrated that 1000 cells in the axial direction and 20 cells in the radial direction for the wall are sufficient to obtain grid-independent results. The test pipe was insulated so an adiabatic condition was

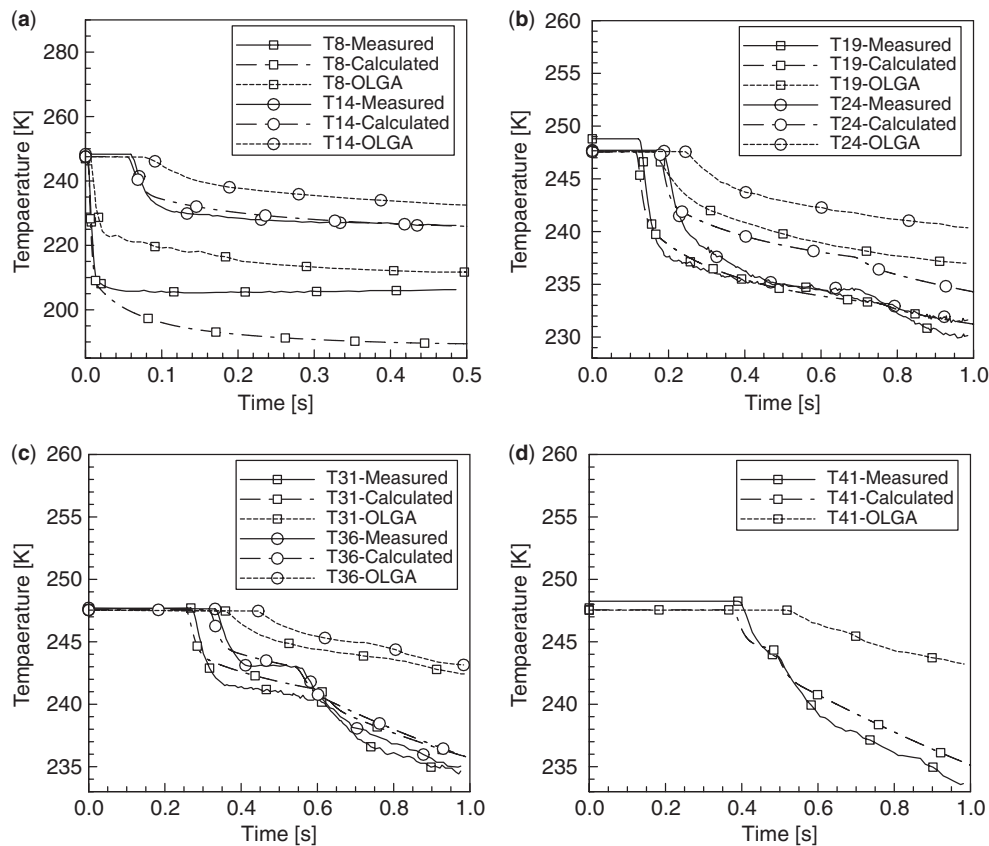


Figure 5. Comparison of temperature-time traces at different locations (case 1)

applied at outer pipe wall. All the simulations started from still and initial temperatures for the wall and fluid were set to be equal.

Figure 4 shows the comparison of pressure-time traces at different measurement locations which are listed in Table 3. As previously mentioned the decompression rate is fast close to the rupture plane (P6 and P7), so the pressure drops quickly before stabilizing at a relatively low value. For locations away from the rupture plane, the decompression rate tends to be slower. For the locations near the close end (P31, P36 and P41), the decompression rates are seen to suddenly accelerate between $t = 500$ ms and $t = 600$ ms. This is thought to be caused by the reflected leading decompression curve. The propagation speed of the leading decompression wave is very accurately predicted by the current simulation and severely under-predicted by OLGA pipeline simulating code (Bendiksen et al., 1991). For all the locations, the current predictions are in reasonably good agreement with the experimental data although relatively larger discrepancies are seen for the locations closer to the rupture plane due to the HEM assumption. The acceleration of the decompression rate at P31, P36 and P41 is also accurately predicted by the current model.

The comparison of temperature-time traces at different locations is shown in Figure 5. Temperature decreases significantly at the locations close to the rupture plane due to the fast decompression rate. Judging from the under-prediction of temperature at the location of T8 which is most likely due to the HEM assumption, the non-equilibrium condition is believed to be significant close to the rupture plane. For the locations beyond T8, the predicted temperature agrees well with the experiment data. For all the locations displayed on the figure, OLGA over-predicts the temperature.

CONCLUSIONS

A CFD based pipeline blowdown model has been developed and validated against experimental data for rich gases, gaseous and dense phase carbon dioxide. The model is based on the HEM assumption for which the two-phase mixture is assumed to be locally in thermodynamic and kinetic equilibrium. It is found that the HEM led to under-predictions of pressure and temperature at locations close to the rupture plane, where non-equilibrium conditions are more profound. Away from the rupture plane, the model performs rather well. Although validation has only been carried out for one-dimensional problems in the present study, the model is based on three-dimensional formulation and has the potential to handle more complex problems involving pipeline networks. The predictions are found to be in reasonably good agreement with the published experimental data. The propagations of both the decompression wave and the reflected wave are accurately captured.

ACKNOWLEDGEMENT

The authors have benefitted from technical discussions with David Jones from Pipeline Integrity Engineers Ltd and

Andrew Cosham from Atkins Boreas during the development of the work.

REFERENCES

- Cosham, A. and Eiber, R.J., 2008, Fracture Control in Carbon Dioxide Pipelines – the Effect of Impurities, *Proc. IPC2008, 7th Int. Pipeline Conf.*, Calgary, Alberta, Canada.
- Cosham, A. and Eiber, R.J., 2007, Fracture Control in Carbon Dioxide Pipelines, *International Conference on Transmission of H₂ and CO₂ by Pipeline*, Amsterdam.
- Botros, K.K., Geerligsa, J., Zhou, J. and Glover, A., 2007, Measurements of Flow Parameters and Decompression Wave Speed Following Rupture of Rich Gas Pipelines, and Comparison with GASDECOM, *Int. J. Pressure Vessels and Piping* 84:358–367.
- Maxey, W., 1986, Long Shear Fractures in CO₂ Lines Controlled by Regulating Saturation, Arrest Pressures, *Oil Gas J.*, 44–46.
- Peng, D.Y. and Robinson, D.B., 1976, A New Two-Constant Equation of State, *Indust. and Eng. Chem.: Fundamentals* 15:59–64.
- Span, R. and Wagner, W., 1996, A New Equation of State for Carbon Dioxide Covering the Fluid Region from the Triple-Point Temperature to 1100 K at Pressures up to 800 MPa, *J. Phys. and Chem. Reference Data*, 25(6):1509–1596.
- Robert C. Reid, John M. Prausnitz and Bruce E. Poling, 1987, *The Properties of Gases & Liquids*, Fourth Edition. McGraw-Hill, Inc., New York, Fourth Edition.
- Mehra, R. and Heidemann, R., 1983, An Accelerated Successive Substitution Algorithm, *Can. J. Chem. Eng.*, 61(4).
- Amsden, A.A., O'Rourke, P.J. and Butler, T.D., 1989, KIVA-II: A computer program for chemically reactive flows with sprays, Technical report LA-11560-MS, Los Alamos National Laboratory.
- Massey, B. S., 1983, *Mechanics of Fluids*, Van Nostrand Reinhold Co. Ltd., Wokingham.
- Beattie, D.R. and Whalley, P.B., 1982, A Simple Two-Phase Frictional Pressure Drop Calculation Method, *Int. J. Multiphase Flow*, 8:83.
- Vesovic, V. and Wakeham, W.A., 1990, The Transport Properties of Carbon Dioxide, *J. Phys. Chem. Ref. Data*, 19(3).
- Fenghour, A. and Wakeham, W.A., 1998, The Viscosity of Carbon Dioxide, *Journal of Physical and Chemical Reference Data*, 27(31).
- Vesovic, V., 2001, Predicting the Viscosity of Natural Gas, *Int. J. of Thermophysics*, 22(2):415–426.
- Fairuzov, Y.V., 2000, Modeling of Conjugate Two-Phase Heat Transfer During Depressurization of Pipelines, *J. Heat Transfer*, 122:99.
- Chen, J.C., 1966, A Correlations for Boiling Heat Transfer to Saturated Fluids in Convective Flow, *Process Design and Development*, 5:322–327.
- Chen, M.M., 1961, An Analytical Study of Laminar Film Condensation: Part 2 – Single and Multiple Horizontal Tubes, *Transactions of the ASME, J. of Heat Transfer*, 83:55–60.

- O'Rourke, P.J. and Amsden, A.A., 1986, Implementation of a Conjugate Residual Iteration in the KIVA Computer Program, Los Alamos National Laboratory report LA-10849-MS.
- Wen, J.X., Xu, B.P. and Tam, V.H.Y., 2009, Numerical Study on Spontaneous Ignition of Pressurized Hydrogen Release through a Length of Tube, *Combust. & Flame*, 156(11):2173–2189.
- Hirt, C.W., Amsden, A.A. and Cook, J.L., 1974, An Arbitrary Lagrangian-Eulerian Computing Method for All flow Speeds, *J. Comput. Phys.* 14:227.
- O'Rourke, P.J. and Amsden, A.A., 1986, Implementation of a Conjugate Residual Iteration in the KIVA Computer Program, Los Alamos National Laboratory report LA-10849-MS.
- Balsara, D. and Shu, C.W, 2000, Monotonicity Preserving Weighted Essentially on-oscillatory Schemes with Increasingly High Order of Accuracy, *J. of Comput. Phys.*, 160:405–452.
- Maxey, W.A., Syler, F.A. and Eiber, R.J., 1975, Fracture Propagation Experiments on 48 inch X 0.72 inch Line Pipe, NEB Public Document NPD-137.
- GASDECOM, 1993, Computer Code for the Calculation of Gas Decompression Speed that is Included. In Eiber, R, Bubenik, T, Maxey, W.A. Fracture Control Technology for Natural Gas Pipelines. NG-18 Report 208, A.G.A. Catalog No. L51691.
- Cosham, A. and Eiber, R., 2008, Fracture Propagation in CO2 Pipelines, *J. Pipeline Eng.*, 7(4).
- Prausnitz, J.M. and Poling, B.E., 1987, The properties of Gases and Liquids, 4th Edition, McGraw-Hill New York.
- Bendiksen, K.H., Malnes, D., Moe, R. and Nuland, S., 1991, The Dynamic Two-Fluid Model OLGA: Theory and Application, *SPE Production Eng.*, 171.